PNAS
www.pnas.org

Supplementary Information for

A bio-inspired stretchable membrane-based compliance sensor

Levent Beker, Naoji Matsuhisa, Insang You, Sarah Rachel Arussy Ruth, Simiao Niu, Amir Foudeh, Jeff B.-H. Tok, Xiaodong Chen, Zhenan Bao*

Zhenan Bao
Email: zbao@stanford.edu

This PDF file includes:

Other supplementary materials for this manuscript include the following:

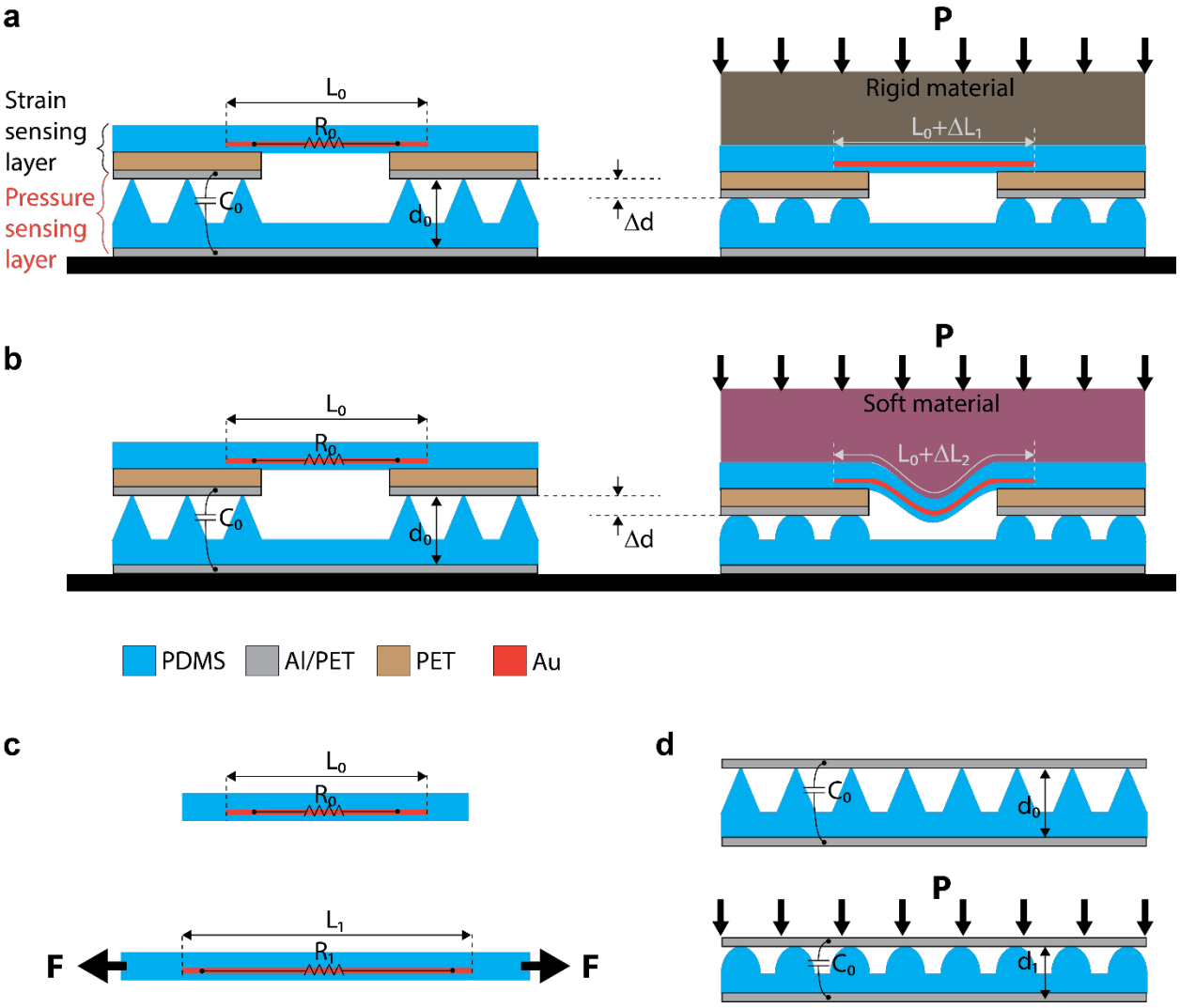

Fig. S1. Operation of the compliance sensor and common strain and pressure sensors. Schematic view of the operation of the compliance sensor that consists of a strain sensor responding to expansion of a material enabled by circular opening and a pressure sensor measuring normal applied pressure during a) contacting to a rigid material, b) contacting to a compliant material. Operation of a typical c) resistive strain sensor that responds to extension; d) capacitive pressure sensor that responds to a normal pressure.

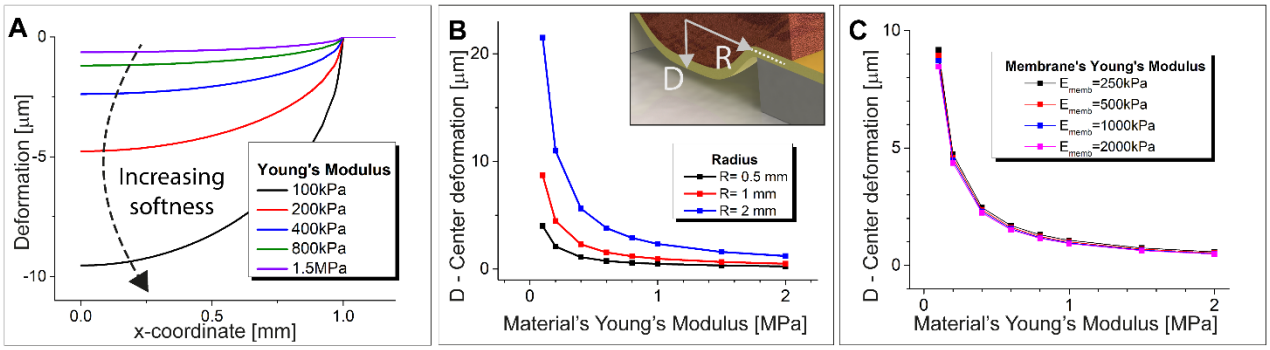

Fig. S2. Finite Element Simulation Results: A) Deflection profile of touched materials of different Young's modulus under 1 kPa of pressure. (x-coordinate refers to the radial axis shown in B) B) Simulation results E) showing effect of radius of the circular opening on center deflection of the membrane structure (subset figure depicts center deflection of the membrane, D, and radius, R. C) showing effect of membrane's Young's modulus on D.

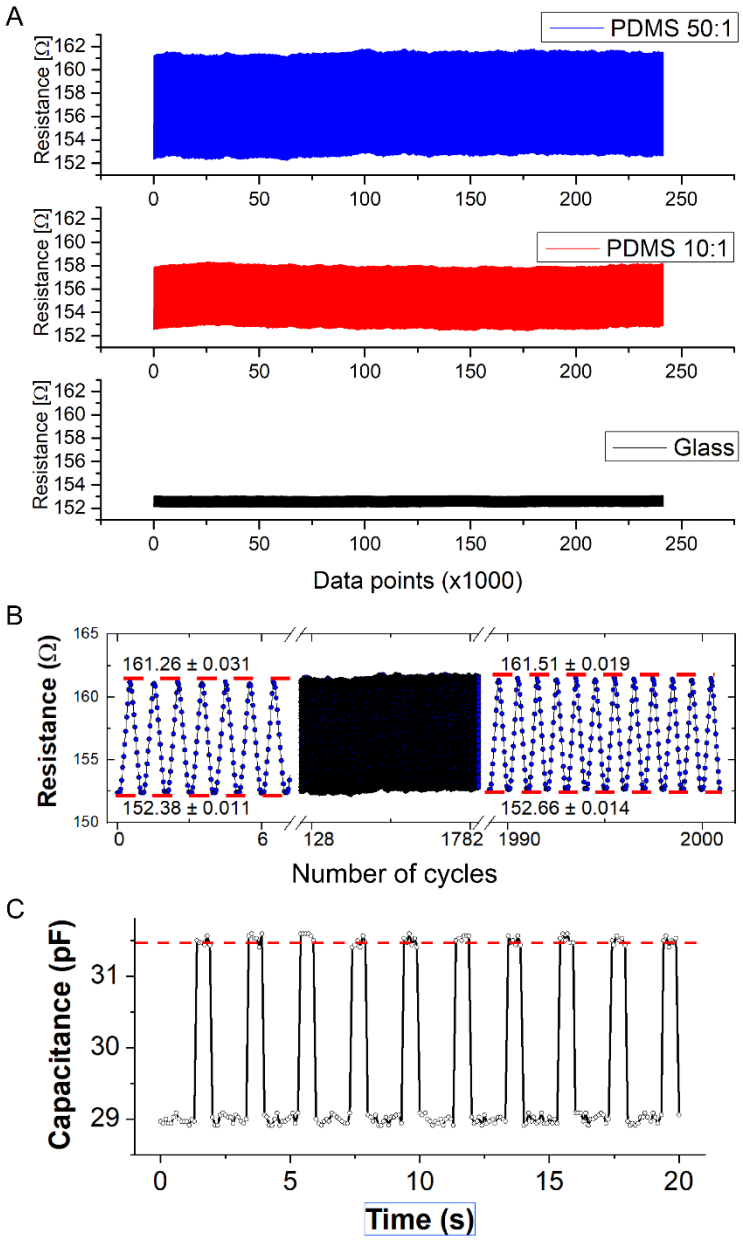

Fig. S3: Cyclic test results of the RMB sensor A) for PDMS (50:1), PDMS (10:1), and glass under 500 cycles with the same applied pressure B) 2000 cycle of PDMS (50:1) response showing first and last few cycles in detail. C) Dynamic loading of pressure sensor for precision and accuracy tests. The measurement error was calculated by $(C_{meas} - C_{ref})/C_{ref}$ x 100%. C_{ref} was found by averaging the capacitance output when applying the dummy mass corresponding to 10 kPa pressure load for 1 min period. Measurement error of 0.56% was obtained for the pressure sensor for the pressure load of 10 kPa.

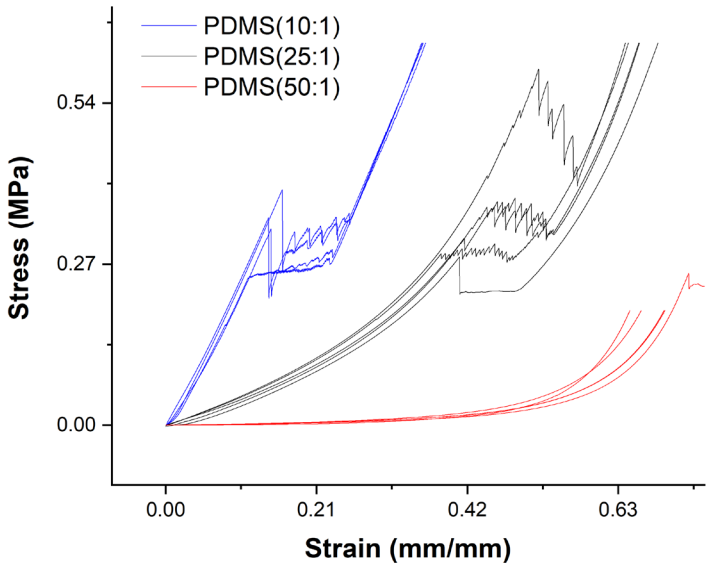

Fig. S4: Uniaxial compression testing of materials: Stress-strain plot of materials that were used during characterization of the compliance sensor. Three different materials were produced using different crosslinker mix ratio. Tested materials had 3 mm thickness and 1 cm^2 of area. 5 different samples from each material were tested.

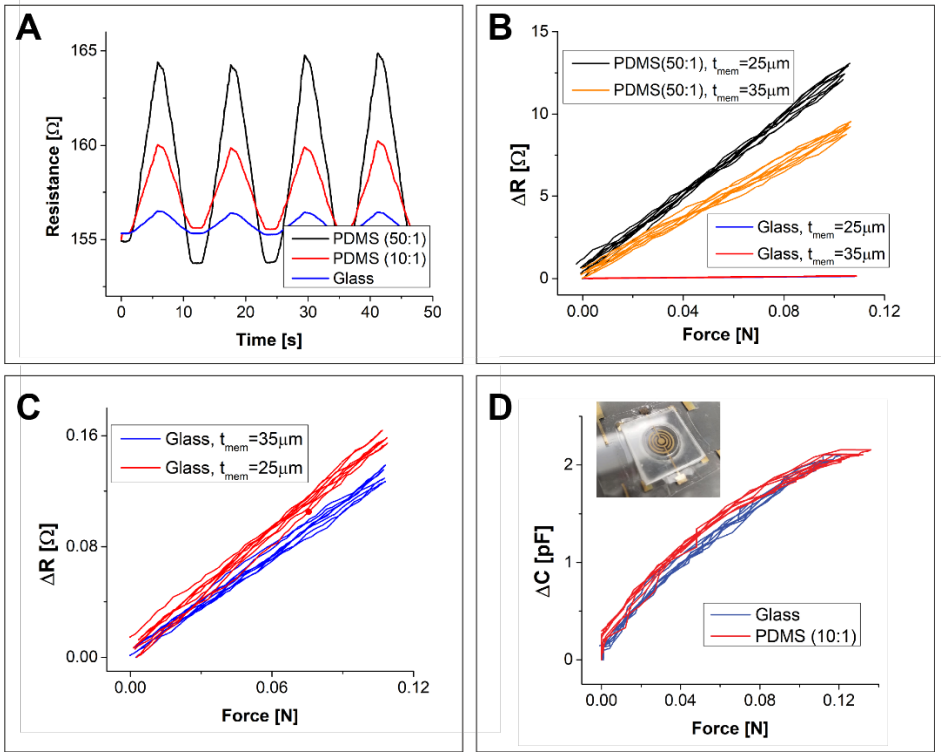

Fig. S5: Characterization of RMB sensor A) Time response of the strain sensor to different materials showing increased sensitivity to compliant materials. Output of resistive strain sensor on membranes of different thicknesses B) when tested with glass and PDMS (50:1); C) close-up view of response of glass showing increased sensitivity of the thinner membrane layer. D) Pressure sensor output of CMB compliance sensor, yielding similar results for objects made up of different materials.

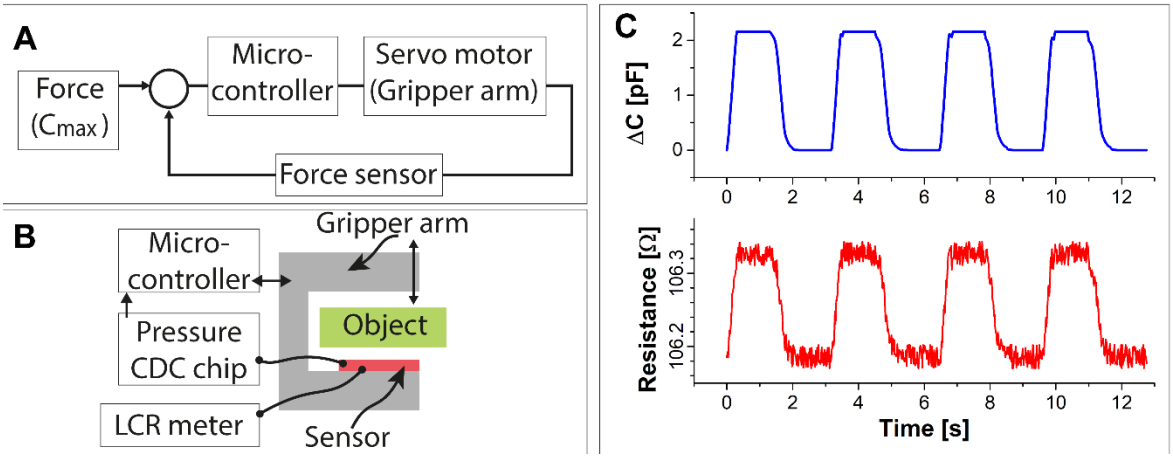

Fig. S6. Integration of compliance sensor to a robotic gripper: A) Control block diagram of the robotic finger. B) Schematic top view of the robotic finger system with integrated compliance sensor for grasping objects. C) Time response of the standalone sensing unit. Top plot shows capacitance output of the pressure sensor layer whereas the bottom plot shows resistance output of the strain sensor layer while touching a glass object.

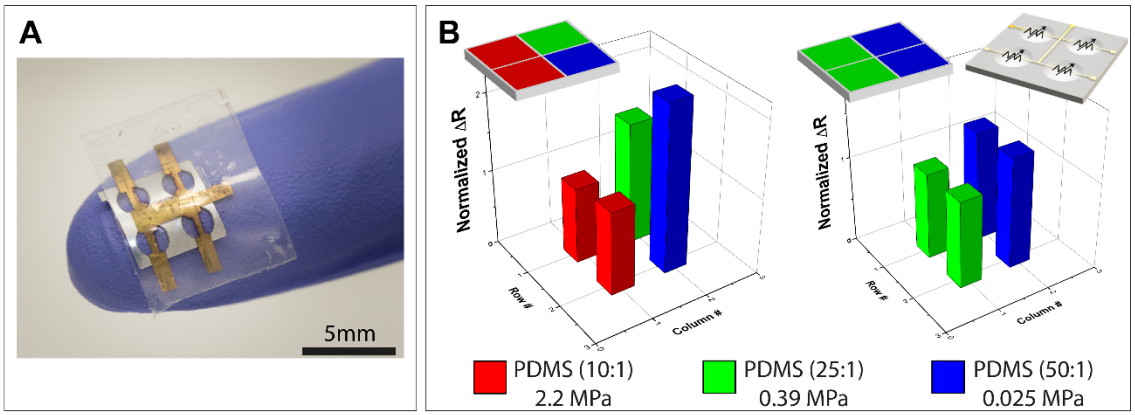

Fig. S7. Demonstration of compliance mapping using a small-form-factor compliance sensor: A) Fabricated 2x2 sensor array placed on finger with. The sensor has a footprint of 1.2×1.2 cm^2 and diameter and pitch of 4.2 mm and 6.9 mm, respectively. Output of the strain sensor when an object B) with three (normalized resistance changes in ascending order 1.00, 1.05, 1.62, 2.18) and two different (normalized resistance changes in ascending order 1.00, 1.03, 1.28, 1.26) materials contacted to sensor with 10 kPa pressure. Subset image shows illustration of the sensor and applied combination of materials. Results show normalized average resistance change of 10 loading cycles. Each RMB sensor pixel has a circular opening of 3 mm with aligned strain sensor of 1.5 mm long and 450 µm width at the center of the opening.

Discussion S1: Multi-modal sensing and coupling of the sensor responses

One of the major challenges of multi-modal sensing is coupling of the sensor responses. In the case of electro-mechanical pressure and strain sensors, the coupling effect is amplified when both sensors structurally overlap due to working mechanism of these sensors, such that applied pressure generates strain or generated strain affects pressure sensor structure, thus its response.

In the work presented here, in order to measure compliance of an object we developed a structure to measure deformation of a certain region of the object per unit applied pressure. This is done through strain and pressure sensors.

To be more specific, a compressive pressure is applied on to a material that is in contact with the compliance sensor. This results in a compliance sensor output with a certain sensitivity in $\Delta R/\Delta C$ (ohms/pF, resistance change ohms/kPa) or $\Delta R/\Delta P$ (ohms/kPa, resistance change per unit applied pressure by using a pre-calibrated pressure sensor). The circular opening on the compliance sensor causes a surface deformation (expansion) on the material which is inversely proportional to the materials stiffness. This deformation is dependent on:

- Material compressive stiffness
    - Young's modulus of the material.
    - Geometrical factors of the material such as thickness and area.
- Radius of the circular opening.
- Stiffness of the strain sensor's membrane (which is negligible compared to materials stiffness due to its thin structure).

As a result, we can measure:

- Compressive compliance, if the thickness of the touched material is unknown.
- Young's modulus of the material, if the thickness of the touched material is known.

In this regard, Fig. 3H shows output of the sensor and calculated compressive compliance of the objects. The compliance sensor proposed here cannot measure thickness of the touched material. However, there are robotic systems with micrometer resolution that are coupled with control systems and able to measure thickness of touched objects. If the compliance sensor is integrated to such systems, then, the sensor could be used to measure Young's modulus of the touched material as shown in Fig. 3G. However, if the sensor is not integrated to such systems and no thickness information is available, then the sensor is able to measure compliance of the touched material.

In order to minimize the coupling between the sensors, here in this work, we introduced circular opening regions specifically for strain sensors which gives us the chance to isolate both sensors to minimize the coupling. This non-overlapping structural design allows decoupled sensor responses up to a certain pressure which can be referred to as operational pressure range.

Fig. 3F shows the multi-modal sensing operation of the compliance sensor. The applied pressure was limited to 10 kPa (maximum operational pressure). The maximum operational pressure can be tailored for specific purposes, such that in general as the size of the sensor shrinks, the maximum operational pressure increases. In this case, the pressure sensor and strain sensor designs are tailored such that they provide linear response within the 0-10 kPa regime. We chose 10 kPa because it is on the order of skin's soft touch sensation. However, as the pressure goes beyond 10 kPa, due to 1) limited gap spacing between the resistive strain sensors membrane and backing layer, 2) large deformations on the membrane yielding non-linear structural behaviors, and 3) structural and material features of the pressure sensor yielding non-linear response, it is

not possible to have reliable and linear sensor responses. Due to these factors, operational pressure is limited to a certain value. After this limit, the strain sensors membrane contacts and sticks to the backing surface and increased pressure does not affect the strain sensor as in the operational range. Similarly, increased loading results in decreased sensitivity in the pressure sensor response as discussed in our group's previous works [1, 2].

Table S1: Mechanical properties of tested objects.

	Object 1	**Object 2**	**Object 3**	**Object 4**	**Object 5**	**Object6**	**Object 7**
Material	PDMS 10:1	PDMS 10:1	PDMS 25:1	PDMS 25:1	PDMS 50:1	PMMA	Glass
L (mm)	3	5	3	5	3	3	3
E (MPa)	2.02	2.02	0.39	0.39	0.0247	2000	70000
A (mm^2)	100	100	100	100	100	100	100
k (EA/L) (N/m)	67333.3	40400	13000	7800	823.3	6.67E+07	2.33E+09
compliance (1/k) (m/N)	1.49E-05	2.48E-05	7.69E-05	1.28E-04	1.21E-03	1.50E-08	4.29E-10
compliance (µm/N)	14.9	24.8	76.9	128.2	1214.5	0.01500	0.00043
Sensitivity (S) (Ω/pF)	2.93	3.4	4.72	5.22	6.5	0.602	0.601

Mov. S1 Demonstration of the compliance sensor on a robotic finger: Compliance sensor placed on a robotic finger and grasps a block of material. Simultaneous recordings of capacitance sensor and strain sensor outputs are shown which are later used to compute sensitivity of the signal to identify the object's compliance.

Fabrication:

Silicon etching: A bare Si <100> wafer with 300nm thermally grown oxide were patterned using photolithography and wet etching (6:1 BOE). Then, oxide was used as a mask during anisotropic silicon etching process. A potassium hydroxide solution (30%, 80ºC) was used for silicon etching followed by oxide stripping using (6:1 BOE). The etched wafer was used as a mold during micro-structured pyramid layer preparation.

Pressure sensor fabrication: To fabricate the pressure sensor layer, a 10:1 mixture of PDMS elastomer (Sylgard 184, Dow Corning) to cross-linker was mixed for 3 minutes at 2000 rpm. Then, a thin layer of resist (S1813, MicroChem) was spin coat as a sacrificial layer on a mold wafer at 5500 rpm for 1 minute followed by soft bake at 90ºC for 2 minutes. Then, the PDMS mixture was poured on the mold wafer and spin coated at 1500rpm followed by curing process at 150ºC for 20 minutes. The sacrificial layer was removed using acetone and the PDMS elastomer layer was transferred to a PET film for handling purposes. The elastomer layer was then laminated in between aluminum (50 nm) coated PET films (25 μm) such that metal coated sides are touching the elastomer to increase sensitivity of the pressure sensor. Finally, the laminated layers were laser cut (Epilog, M2 Fusion) using CO2 laser (a power of 15W and frequency of 15 Hz) and circular openings for membranes are patterned.

Membrane-based resistive sensor fabrication: First, Dextran (Sigma Aldrich, Mw 100,000) sacrificial layer was spin coated on glass slide (2" x 3") followed by spin coating PDMS with desired mixture ratios (10:1, 25:1, or 50:1) and cured at room temperature for overnight. A shadow mask was prepared by CO2 laser cutting a Kapton tape with desired resistive sensor pattern. Then, Cr/Au/Cr (Cr, 4 nm with 0.1A/s, Au, 50nm with 2A/s) metal was evaporated on the elastomer through the shadow mask. The sacrificial layer was dissolved in water and membrane layer was easily transferred to a PET temporary holder. Finally, the membrane layer was aligned to the pressure sensor such that strain sensitive region is placed at the middle of the circular opening of the pressure sensor.

Membrane-based capacitive sensor fabrication: The capacitive sensor fabrication is similar to resistive sensor except a second layer of PDMS was spin coated on top of the electrode layer to provide encapsulation. After peel off process, it was aligned and laminated on top of the pressure sensor.

Characterization:

An automated high-precision vertical stage was used to control applied pressure on the sensor. A custom software controlled the vertical stage and recorded capacitance or resistance of the sensors as well as force gauge readings, as shown in SI Appendix, Fig. S5A. Materials with different modulus and controlled thickness were placed on top of the sensor and contacted to the force gauge to measure applied force during loading. As the moving stage elevates, the pressure applied on the material increases and the force gauge records the applied force which is recorded by computer to control the moving stage.

Robotic gripper demonstration: The fabricated sensor was mounted on one side of a robotic gripper robot's fingers (Lynxmotion Little Grip Kit, Robotshop). The sensor was connected to an LCR-meter (Agilent E4980A) for resistance measurements and monitored through a custom-built software through a computer. A capacitance-to-digital converter microchip (FDC1004, Texas Instruments) was connected to the pressure sensor for capacitance measurement. The chip was connected to the micro-controller and monitored through a computer. The robot finger was also connected to the controller (Arduino Uno, Rev 3) and a feedback loop was developed using microcontroller's software. PDMS mixtures with different ratios were prepared and molded to have 4 mm of final thickness. Finally, materials were placed in between the gripper fingers for grasping tests.

References

[1] S. Ruth, L. Beker, H. Tran, V. Feig, N. Matsuhisa, Z. Bao, “Rational Design of Capacitive Pressure Sensors Based on Pyramidal Microstructures for Specialized Monitoring of Biosignals”, Advanced Functional Materials, 1903100, 2019.

[2] Tee, B. C., Chortos, A., Dunn, R. R., Schwartz, G., Eason, E., & Bao, Z. (2014). Tunable Flexible Pressure Sensors using Microstructured Elastomer Geometries for Intuitive Electronics. Advanced Functional Materials, 24(34), 5427-5434. doi:10.1002/adfm.201400712